Latin American Journal of Solids and Structures
www.lajss.org

Effect of Thermal Residual Stresses on Buckling and Post-Buckling Properties of Laminated Composites Perimetrally Reinforced

Abstract

Several mechanical properties can be affected by the occurrence of residual stresses due to curing, and their effects are more pronounced in laminated composites. The effect of the thermal residual stresses on the buckling and post-buckling properties of perimetrally reinforced laminated composites is experimentally characterized. Carbon/epoxy laminates were prepared using two different techniques. One group of laminates was prepared by co-curing the reinforcement at 177 °C. The second group of laminates was prepared by secondary bonding of the reinforcement to the laminate at room temperature (22°C). Topogrammetry equipment was utilized in order to determine the buckling and post-buckling properties of these two groups of laminates. A numerical model was achieved using commercial software for comparison with the experimental results. Suitable accuracy was observed when comparing experimental and numerical results. The co-cured laminates developed considerably higher critical load for buckling values than those obtained for laminates produced with secondary bonding at room temperature. The experimental and numerical results of this study demonstrate the importance of curing-induced thermal residual stresses on the mechanical behavior of laminate composites.

Keywords

Composites, laminates, thermal stresses, topogrammetry, buckling, post-buckling

Martha L. Sánchez Cruz [a]
Julián Carrillo [b]
Sergio F. Muller de Almeida [c]

[a] Universidad Militar Nueva Granada Carrera 11 101 80, Bogotá, Colombia, martha.sanchez@unimilitar.edu.co
[b] Universidad Militar Nueva Granada Carrera 11 101 80, Bogotá, Colombia, wjcarrillo@gmail.com
[c] Instituto Tecnológico de Aeronáutica, Praça Marechal Eduardo Gomes, 50, São Jose dos Campos Brasil, frascino@ita.br

http://dx.doi.org/10.1590/1679-78251828

Received 24.07.2015
In revised form 07.12.2015
Accepted 11.12.2015
Available online 05.01.2016

1 INTRODUCTION

The application of laminated composites is becoming increasingly important in mechanics, aeronautics, and engineering, mainly in those projects that have structural requirements such as strength, durability and low weight. In these projects there is an important relation between the geometry of the elements, the adequate selection of their constituent materials, and the process of manufacturing selected for the confection of material.

For proper design of composite structures, both the performance requirements and the possible appearance in the structure of thermally-induced stresses should be considered, which may substantially affect their mechanical behavior, positively or negatively. Due to the non-homogeneity of the material, thermally-induced stresses are always present in the manufacturing processes of fibrous polymeric composites. This concept was introduced by Parlevliet et al. (2006). These stresses arise because of the anisotropy of the material, which can be analyzed at the micromechanical level when considering the difference between the coefficient of thermal expansion and the modulus of elasticity of the fibers and the matrix that make up the composite material, and at the macro-mechanical level considering the expansion or contraction of the different laminas that make up the laminate. This expansion or contraction depends on the orientation of the laminas with respect to a reference system. Reports of this effect were presented by Gascoigne (1994), Hosseini-Toudeshky and Mohammadi (2009), and Ersoy and Vardar (2000).

Over the years, several studies have reported that the presence of residual stresses associated with the curing process of composite materials can negatively affect the performance of the composite material, principally its dimensional stability, and additionally can generate delamination, causing the premature failure of the material. An example of these investigations is that presented by Kim et al. (2006). Tay and Shen (2002) report values for buckling and post-buckling of laminated composites and present a prediction of their delamination process in presence of residual thermal stresses. The evaluation of the effect of curing stresses on interlaminar delamination crack growth behavior in fiber-reinforced polymeric composites was presented by Pradhan and Panda (2006). In this paper, results are developed for elliptical delamination embedded between plies of different orientations in the analyzed laminate. The results presented in this investigation show that the residual thermal stresses that occur during the manufacturing process of laminated composites significantly affect the onset and growth of delamination. Fen et al. (2015) report the effect of the hygrothermal condition on buckling and post-buckling performance of CCF300/5228A aero composite stiffened panel under axial compression. The experimental tests were conducted on unaged and aged composite stiffened panels. One of the most important results presented in this paper is the difference in the bending direction of mid-panel buckling for two case studies at the same position of the panel, which shows that the hygrothermal condition greatly influences the bending direction of the buckling.

Other important effects of temperature on the behavior of composite materials can be found in the technical literature. Aktas et al. (2009)show that the impact-test temperature has a significant effect on the compression and after-impact strength of the laminates. The laminates used for this paper were obtained for two-ply sequences at $[0°/90°/0°/90°]_S$ and $[0°/90°/45°/45°]_S$ with vertical impact damage for the impact-test temperature. In this study, glass/epoxy composite plates were used. The plates were subjected to various impact energies at room temperature and high temperatures between 40°C, and 100 °C.

The impact and post-impact response of laminated beams at low temperatures was report by Ibekwe et al. (2007). The results reported by the authors have contributed to the understanding of the damage mechanism in laminated composites. The influence of environmental temperatures on the impact damages and on the residual compressive buckling stress and Young modulus was evaluated for unidirectional reinforced glass fiber and cross-ply laminated composite beams, and novel results were presented.

Recent studies have focused on reducing the adverse effects of the thermal residual stresses on the performance on composites materials (Kim et al. (2006), Kim et al. (2013), Shokrieh et al. (2014)).

New research proposed modifications to the curing process of the composite materials. In this sense, Kim et al. (2006) proposed a curing method based on heating and cooling stages, achieving a reduction of up to 30% of thermal stresses in thick-walled cylindrical composites, while Kim et al. (2013) show a monitoring system using dielectrometry and Brag networks based on the use of sensors to control the cure cycle in the manufacturing process. The proposed method allows reducing the thermal stresses in reinforced composites with carbon fibers.

Currently, some researchers have proposed modifications to the curing process in order to minimize the negative effect of residual thermal stresses. At present, it has been found that the use of nano additives with a negative coefficient of thermal expansion can reduce the presence of residual thermal stresses in polymeric composites. Shokrieh et al. (2014) studied the effects of thermal residual stresses on the mechanical properties of polymeric composites using carbon nanotubes as additives. The results obtained show a significant reduction of residual stresses at a micro- and macro-mechanical level.

Almeida and Hansen (1999, 2002) introduced the idea of using the curing stresses that occur during the manufacture of laminated composites to improve the mechanical performance of reinforced laminates. They numerically demonstrated that residual thermal stresses might be used to increase the natural frequency of free vibration and the critical load buckling of reinforced laminates.

Traditional methods such as the Riks method and arc length method are widely known and applied in the study of the mechanical behavior of thin laminates. Taylor et al.(2014) presented a comparative analysis of the application of these methods and the dynamic relaxation method in the numerical simulation of the mechanical behavior of thin laminates, showing results demonstrating the robustness of the dynamic relaxation method and its applicability in problems associated with the analysis of the elements in a condition of static equilibrium. Nunes and Almeida (2005)analytically evaluated the post-buckling behavior of a composite material in the presence of thermal residual stresses. For this study, the Crisfield arc-length method was used, with MSC. Nastran® software.

To experimentally evaluate the effect of residual thermal stress on the performance of reinforced laminates, Sanchez and Almeida (2007) presented a study that is a first approach to the experimental characterization of reinforced composites. In this paper, preliminary values for stiffness were obtained for plates with varying typology of reinforces. These theoretical and experimental studies provided motivation for the present paper, which numerically and experimentally evaluated the effect of residual thermal stress on the post-buckling and buckling of laminates reinforced around their perimeter.

For the development of this study, plates with reinforcements located around their perimeter were analyzed. The selection of the type of reinforcement was based on previous papers in which analytical results for laminates with this type of reinforcement was presented(Sanchez and Almeida (2013), Almeida and Hansen (2002), and Nunes and Almeida (2005)).The plates were prepared with the pre-impregnation method described by Besednjak (2005), using a base fabric composed of four laminas with orientation [(0,90)]s, on which are placed reinforcements formed by four laminas oriented at 90° vertically and 0° horizontally. To induce residual thermal stresses, two study groups were created by varying the technique employed in the gluing during the curing process of the reinforcements. For each of the study groups, the value of the critical buckling load, the configuration of the first three

modes of linear buckling behavior, and the behavior of the post-buckling stage were determined. To develop the experimental procedure, an optical technique was used (Fantín (1999)). The applied technique allows the determination of the deformation out of the plane and its use for the analysis of buckling and post-buckling behavior for the plates studied.

2 THEORETICAL ANALYSIS

The theoretical formulation used for the study of composite laminates subjected to buckling conditions can be divided into three stages of analysis, according to Nunes and Almeida (2005) and Sanchez et al. (2015).

2.1 Analysis of the Thermal Problem and Establishment of Initial Conditions

Applying the classical theory of lamination to the study of composite laminates, it is possible to express the relationship between the internal forces and deformations that occur in a material in the presence of temperature effects without external forces, which can be expressed according to Equation 1.

$$\{N^T\} = [A]\{\varepsilon^0\} + [B]\{k\} \tag{1}$$

where:
$\{N^T\}$ is the vector of thermal resultant stresses
$\{\varepsilon^0\}$ is the vector that represent a deformations in the middle plane
$\{k\}$I is the vector that represent e curvature in the middle plane
$[A]$ is the stiffness matrix
$[B]$ is the coupling matrix

Since the resulting vector of the thermal stresses depends on the stiffness, position, and deformations in each of the laminas, it is possible to write Equation 2:

$$\{N^T\} = \sum_{k=1}^{n} (h_k - h_{k-1})[\bar{Q}]_k \{e^T\}_k \tag{2}$$

where:
n is the number of laminas
h_k, h_{k-1} are the coordinates of each one of the laminas with regard to middle plane of laminate
$[\bar{Q}]_k$ is the stiffness matrix for a lamina k
$\{e^T\}_k$ is the vector of thermal strains

According to Nunes and Almeida (2005), Palerosi (2006), and Andrade (2002), whereas the stiffness and coupling matrix are the average of the result of the one of the laminas, it is possible to find an expression to determine the stresses in the laminate (see Equation 3).

$$\{\sigma\}_k = [\bar{Q}]_k\{\varepsilon\} - [\bar{Q}]_k\{e^T\}_k \tag{3}$$

where:
$\{\sigma\}_k$ are the stresses in the laminate
$\{\varepsilon\}$ are the strains in the laminate

Once established the thermal stresses and the associated deformation, it is possible to apply an equation for the potential energy as a function of the stiffness matrix of each lamina and their thermal deformation to a coordinate system whose origin is located in the center of laminate. The displacements associated with the laminates in their equilibrium position are those that minimize the potential energy. This leads to a system of nonlinear equations whose solution involves more than one configuration of stable equilibrium, which can be analyzed from the second variation of the potential energy.

2.2 Pre-Buckling Analysis

Considering the symmetry of the laminate, the stresses for any point of the buckled plate can be determined according to Equation 4:

$$\begin{Bmatrix} \bar{\sigma}_x \\ \bar{\sigma}_y \\ \bar{\sigma}_{xy} \\ \bar{\sigma}_{xz} \\ \bar{\sigma}_{yz} \end{Bmatrix} = \begin{bmatrix} [\bar{Q}_M] & [0] \\ [0] & [\bar{Q}_S] \end{bmatrix} \begin{Bmatrix} \bar{\varepsilon}_x \\ \bar{\varepsilon}_y \\ \bar{\varepsilon}_{xy} \\ \bar{\varepsilon}_{xz} \\ \bar{\varepsilon}_{yz} \end{Bmatrix} + \begin{Bmatrix} \bar{\sigma}_x^0 \\ \bar{\sigma}_y^0 \\ \bar{\sigma}_{xy}^0 \\ \bar{\sigma}_{xz}^0 \\ \bar{\sigma}_{yz}^0 \end{Bmatrix} + \begin{Bmatrix} \bar{\sigma}_x^R \\ \bar{\sigma}_y^R \\ \bar{\sigma}_{xy}^R \\ \bar{\sigma}_{xz}^R \\ \bar{\sigma}_{yz}^R \end{Bmatrix} \tag{4}$$

where:
$\{\bar{\varepsilon}\}$ represent the lineal and non-lineal components of the strains

Numerical analysis of buckling behavior presented in this paper was done using the software ABAQUS®, from extraction of the eigenvalues. According to the Abaqus 6.5.1Theoretical Manual (2005), the obtaining of the eigenvalues for the buckling prediction requires a linear perturbation to determine the incremental stresses. When the analysis does not require the inclusion of geometric nonlinearity, the stiffness matrix used in this static perturbation analysis is the tangent elastic stiffness; otherwise, initial stress and load stiffness terms due to the preload are included.

2.3 Post-Buckling Analysis

According to classical theory, analysis of the post-buckling of composite structures can be regarded as a nonlinear quasi-static analysis, where the load is increased incrementally, identifying the point instability of the structure and its behavior once that point is exceeded. To solve the problem, the method of relaxation dynamics is used. This iterative method starts from the consideration that the equilibrium equations for a discrete medium can be derived using centered finite differences, which

can be determined from the general equilibrium equation expressed in Equation 5 (Nabaei (2013), Donadon et al. (2010), Abaqus 6.5.1 (2005)):

$$\{F(\{u\})\} = \{f\} \tag{5}$$

where:
{F} is the internal loads vector
{u} is the vector of displacements
{f} is the vector of external loads

For non-lineal systems, the internal load vector is raised incrementally and the stiffness matrix is solved step-by-step according Equations 6 and 7 (Abaqus 6.5.1 Theoretical Manual (2005)):

$$\{\Delta F\} = [K(\{u\})]\{\Delta u\} \tag{6}$$

$$[K(\{u\})]\{\Delta u\} = \{f\} \tag{7}$$

where:
[K({u})] is the secant stiffness matrix

The above equation represents a system of simultaneous equations whose solution can be obtained according to Equation 8:

$$\{u^*\} = [K]^{-1}\{f\} \tag{8}$$

where:
{u*} is the solution for the system of equation proposals
$[K]^{-1}$ is the inverse of the stiffness matrix
{f} is the vector of external loads

3 EXPERIMENTAL PROCEDURES

Symmetric carbon/epoxy reinforced laminates were used in this study to assess the influence of thermal residual stresses on the buckling and post-buckling behavior of perimetrally reinforced laminated plates. The laminated plate for the analysis was [0/90]s, reinforced with two carbon/epoxy prepreg layers. The reinforcement was symmetrically placed around its perimeter.

For the study, it was considered that during the processing step no internal stresses are generated in the material and that the residual thermal stresses are the result of the cooling process to the service temperature, a residual compression in the reinforcement and a residual stress in the base fabric being generated during this step.

Two case studies were considered in this research: In the first case, the laminate and its reinforcements were manufactured separately and attached at the service temperature, producing reinforced laminates without thermal residual stresses, for which "FB" nomenclature was used. For the second case, both the laminate and the reinforcements were processed simultaneously at a temperature of

177°C, and then were cooled to the operating temperature (22°C), thereby inducing the occurrence of residual thermal stresses in the material. The "FC" nomenclature was used for this case.

In Table 1, the lay-up sequence of laminates is shown. In this table, CT and CF symbolize a carbon/epoxy unidirectional tape and a carbon/epoxy prepreg layer, respectively, and the subscript S represents the symmetry of laminate.

Laminate	Orientation
L1	$[(0,90)^{CF}]_S$
L2	$[(0/90)2^{CT}/(0,90)^{CF}]_S$
L3	$[904^{CT}/(0,90)^{CF}]]_S$
L4	$[04^{CT}/(0,90)2^{CF}]_S$

Table 1: Lay-up sequence of laminates.

The plates were produced via manual lamination by an aerospace company with extensive experience in the manufacture of this type of materials. The prepreg T7G190-12"-F584-21: 34% was used. The cure process was a cycle in an autoclave with two temperature levels, carried out in accordance with the suggestion of the material's manufacturer. No post-curing process was used, since the manufacturer of the material does not recommend it.

The fabric used comes from the manufacturer Hexcel Composites under the designation T / G190-12"-F584-21: 34 %. This designation indicates fiber type T7G190 impregnated in a system of resin F584-21, with nominal mass content of 34%. The properties of the constituent materials were determined from the catalogs of the companies that provided the material used. Table 2 shows the properties of the materials. In this table, CT and CF symbolize a carbon/epoxy unidirectional tape and a carbon/epoxy prepreg, respectively. Geometry and dimensions of the square plates are shown in Figure 1.

Property	Carbon epoxy prepreg (CF)	Tape (CT)
Longitudinal modulus of Young, MPa	66000	130100
Transversal modulus of Young, MPa	66000	9400
Poisson's coefficient	0.05	0.30
In plane shear modulus, MPa	4600	5800
Transverse shear modulus, MPa	3360	3360
Longitudinal thermal expansion coefficient, $°C^{-1}$	1.79e-06	-0.17e-06
Transverse thermal expansion coefficient, $°C^{-1}$	1.79e-06	23.10e-06
Ply thickness, mm	0.350	0.170
Density, g/cm^3	1.56	1.56

Table 2: Properties of constituent's materials.

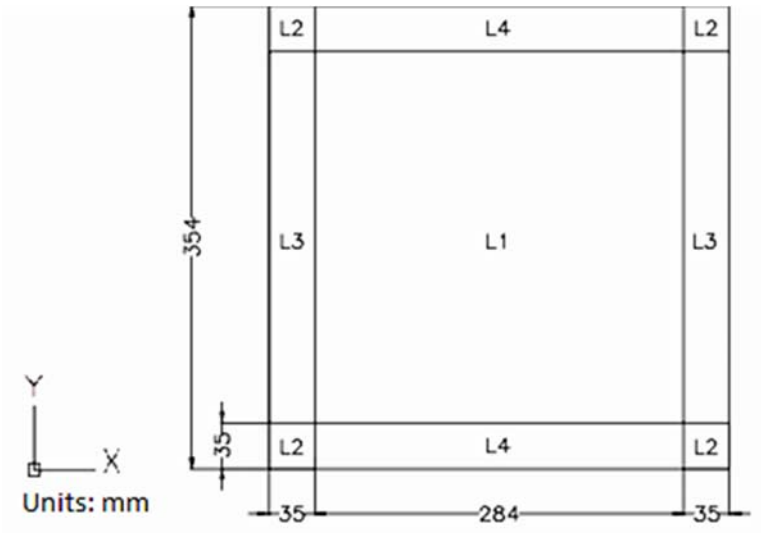

Figure 1: Dimensions of the reinforced plates (L is the lamina with orientation according Table 1).

The laminates used in this paper were made simultaneously, the vacuum bag was applied, and then all the plates were cured with the same curing process in an autoclave. The use of the same conditions for the manufacturing process and the simultaneous elaboration of the plates decrease the uncertainties and normalize the effects of the processing, enabling a consistent comparison between the results obtained in the study.

The 5900 Series Universal Testing Instruments was used in the experimental study. An Instron machine, having a load cell of 30 kN, was used for assessing the experimental analysis of the buckling. The test setup of the plate is showed in Figure 2(a). A piece of aluminum was designed for coupling the load cell to the steel frame in which the plate was supported. The optical measurement system shown in Figure 2(b) was used to determine the transverse displacements occurring on the plate due to the compression load.

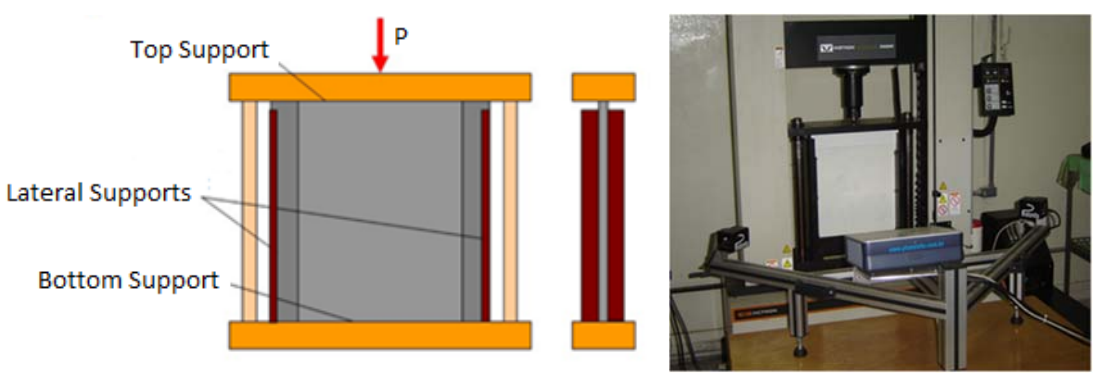

(a) Device (b) optical measurement system

Figure 2: Buckling test setup.

The influence of the curing stresses on the mechanical properties of composites can be analyzed using optical procedures. For instance, topogrammetry is an optical procedure that combines the topometric and photometric procedures for determining displacements on surfaces. This method is based on the establishment of the geometric relation between two images captured from two different perspectives for the same object. The orthogonal patterns of a grid are projected into the surface from light emitted from a projector. The patterns obtained are used to map the geometry of the surface. The phase displacement technique is used for assessing the four phase maps. Such maps contain the information for correlating the images of the two digital cameras with the physical point to be measured. This optical technique allows calculating three coordinate axes using standard triangulation techniques. The sequence of optical procedures is shown in Figure 3. The resultant image provided by the experimental procedures is shown in Figure 4.

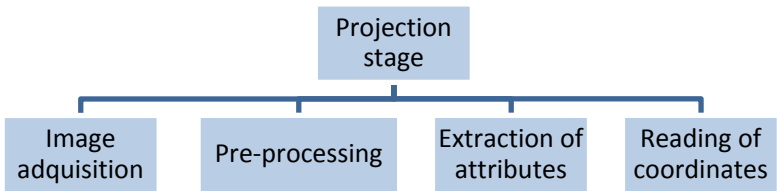

Figure 3: Sequence of optical procedures.

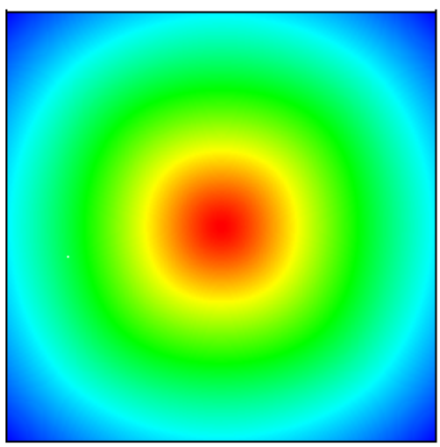

Figure 4: Resultant image of optical procedures.

The experimental technique selected for the development of the experimental test was the application of displacements applied consecutively at intervals of 0.2 mm at a speed of 1 mm/min. This allowed the capture of the images for several intervals of displacements. The images obtained were processed in order to determine the out-of-plane displacements, caused by compression of the plate. The images were subsequently processed using TPLA40012® software. The temperature in the laboratory ranged between 22°C and 25°C.

4 NUMERICAL MODEL

To perform the numerical approximation, a model using the commercial software ABAQUS® was used. The analysis was divided into two stages: verification of performance during step buckling behavior and verification at the post-buckling stage.

The linear perturbation analysis option available in the software was used to determine the linear buckling behavior. This type of analysis provides a response for linear problems, in which only the elastic properties of the material are considered. The option of "Prediction of eigenvalues of buckling", in which a field of initial temperature was set to induce thermal stresses in the model was used. This method allows evaluating the behavior of plates under the effect of residual thermal stress, and is useful for determining the critical buckling load.

For the post-buckling stage, the module "Explicit dynamic analysis" was used. This method performs a large number of small-time increments using the explicit central-difference time integration rule. According to the Abaqus 6.5.1 Theoretical Manual (2005), the application of small increments can be an advantage, because it reduces the number of iterations, does not require the tangent stiffness matrices to be formed, and simplifies the treatment of contact.

A linear perturbation was applied, and a thin shell quadratic element working at double curvature was used in the numerical models. The mesh layout used for modeling was based on the convergence of the value of the critical buckling load obtained in plates without residual stresses. Different mesh sizes of the structure (4000, 8000, 12000, 16000 and 20000 elements) were assessed by varying the number of elements in a ratio equal to 4. The error of the convergence test for this type of plate was 0.02%. Based on the convergence test, and considering that the processing time evidently was not increased, a mesh of 20000 elements was chosen. The results of the convergence test are presented in Figure 5.

Models with and without residual stress were elaborated in order to evaluate the effect of thermal residual stresses. The boundary conditions considered in all simulations are shown in Figure 6, in which U are the displacements, UR are the rotations, and the subscripts are related to the reference system adopted. A unitary loading line across the top edge of the plate was applied to simulate the compressive loading. Thus the buckling load for the first three buckling modes is obtained by multiplying the eigenvalue obtained by the width of the plate.

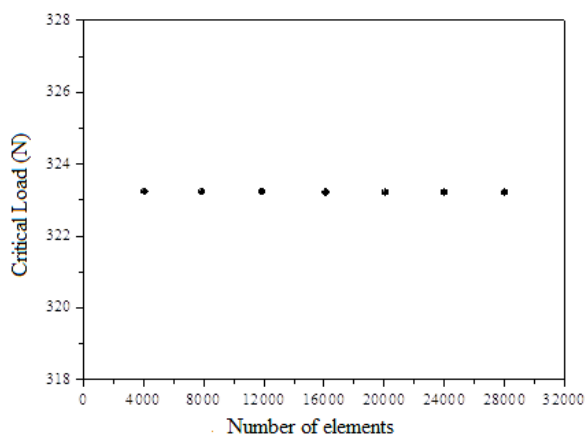

Figure 5: Results for convergence test.

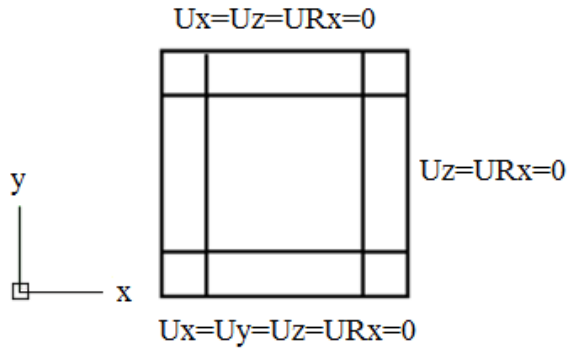

Figure 6: Boundary conditions for the simulations.

To evaluate the critical buckling load in the plates with thermal residual stresses, a uniform temperature field in the unrestrained support plates was introduced in the numerical model. Residual stresses caused by the presence of the temperature field are considered in the linear buckling analysis. A geometrically imperfect numerical model was developed using CATIA® software to determine the effect of geometric nonlinearity. The coordinates extracted from the images of reference provided by the optical measurement equipment were used to determine the coordinates of the vertices of the plate. The geometrically imperfect design was imported into ABAQUS®, and a row of unitary compressive load was applied at the upper edge of the plate to obtain the eigenvalues.

The type of analysis performed in the study of post-buckling behavior was a dynamic analysis of the explicit type previously described. This analysis uses S4R-typeelements, which are linear thin shell elements, four-node, double curvature and hourglass control. To evaluate the effect of geometric nonlinearity introduced by the occurrence of thermal strains, two types of analyses were considered. An ideally perfect plate was considered in the first analysis. By applying a compressive load on this type of element, deformations occur only in the plane of the plate. Such deformations are not observed in practice, because the application of a temperature field during the manufacturing process causes warping of the plates and the appearance of strains out of the plane. To solve the problem of geometric nonlinearity, different values of transversal displacement were applied. From the results obtained, it was decided to use the value of such displacement equal to the thickness of the plate, since small values do not allow the plate to leave its equilibrium state. The transverse displacement is applied before compression. The second analysis used, in order to include the effect of geometric nonlinearity in the post-buckling analysis, was the utilization of a geometrically imperfect model previously designed with CATIA® software. The results obtained in both case studies were very similar; for this reason, using the model designed by CATIA® software was considered for this paper, because the resulting geometry is more representative of the real conditions of the experimental study.

5 RESULTS

The main results obtained in the linear buckling state and in the post-buckling state are presented and discussed below.

5.1 Linear Buckling State

A unitary load line was applied at the upper edge of the plate to predict the critical buckling load. The first three eigenvalues were found to be 1.25, 1.63 and 2.59, which determine critical buckling loads of 442 N, 577 N and 917 N, respectively. These results can be contrasted with those presented by Nunes and Almeida (2005), in which values for the critical load of buckling between 200 and 400 N were reported for plates with reinforcements of different width located all along their perimeter. On the other hand, the results presented are in agreement with those reported by Sanchez et al. (2015) for the evaluation of composites with lateral reinforcements, showing the influence of the type of reinforcement on the mechanical behavior of structural element. The first three modes of shapes of buckling that were numerically determined are shown in Figure 7.

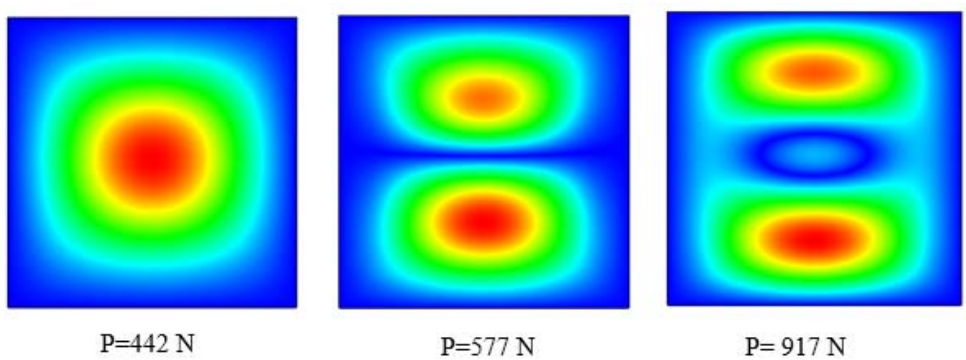

Figure 7: Shapes of buckling. P is the critical load.

Values of the critical buckling load between 280 N and 380 N were obtained from the experimental studies. The percentage of error between the maximum values of critical load obtained experimentally and numerically was approximately 15%. This low value of error demonstrates that the experimental results show an acceptable compatibility with the result obtained in the numerical model. Figure 8 shows the load values obtained using plates cured at 22°C. Figure 9 shows the load values obtained using plates cured at 177°C.

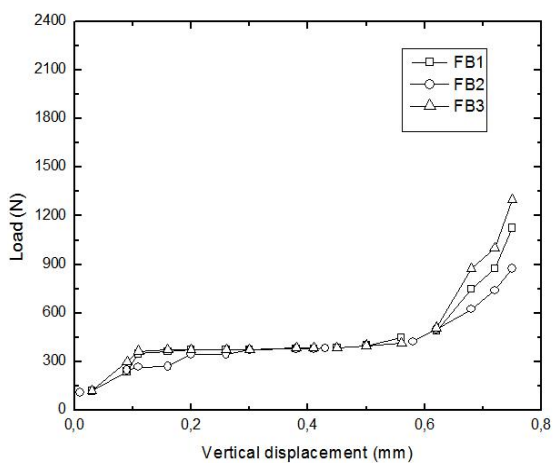

Figure 8: Critical buckling loads determined experimentally for plates cured at 22°C.

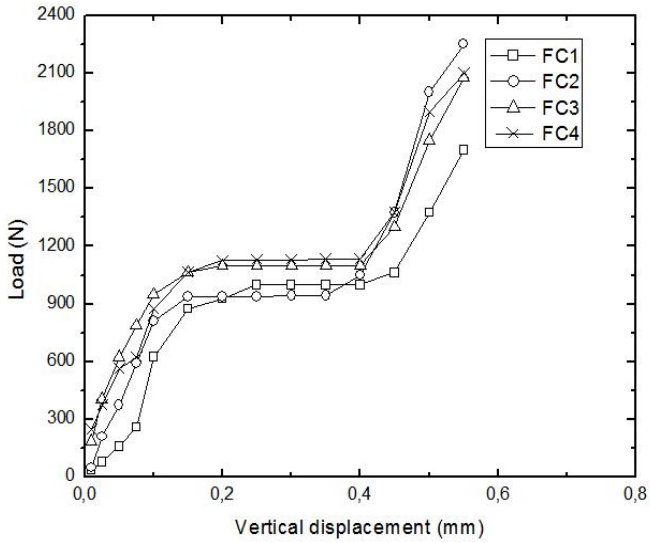

Figure 9: Critical buckling loads determined experimentally for plates cured at 177°C.

A uniform field temperature of 177°C was induced in order to evaluate the effect of residual thermal stresses using a model designed with CATIA® software. This scenario is similar to the real characteristics of the test plates. According to the results of the numerical model, by inducing the presence of residual thermal stresses in the laminate, the critical load increases to 1473 N, whereas the experimental results show values between 950 and 1200 N, for an error of 18%. Similar results were obtained analytically by Nunes and Almeida (2005), who report that for reinforcement plates 36 mm wide critical buckling load is increased from 274.7 to 946 N when the thermal gradient is 150°C.

To verify the effect of the curing stresses in the modal shape of buckling, numerical models were developed for intermediate values of temperature (100 °C and 150 °C).Figures10,11, and 12show the shape of the first three modes of buckling for each of the temperatures analyzed with the numerical model. The results show that the load increase is not proportional. This behavior is most noticeable for the second and third modes of buckling at a temperature of 177°C. A change in the characteristic shape of these modes can also be observed.

From the results shown, it is possible to perceive a modification of the shape of modes and an asymmetric behavior of the buckling modes by inducing residual thermal stresses. This factor could be associated with the inclusion of the thermal problem in the numerical model, in which the plate with completely unrestricted supports was subjected to a uniform temperature field that causes a nonlinearity in the material before the mechanical stresses are applied. It is also important to emphasize that upon observing Figure 6, it can be seen that the conditions of shape established in the analysis restrict the vertical displacements only along the lower edge of the element studied. Similar results were obtained after Sanchez et al. (2015) analyzed plates with lateral reinforcements, showing a change in the mode shape and an asymmetry which increased with the temperature gradient. However, it is important to note that a precise analysis of the cause of this behavior requires a thorough analysis that is beyond the scope of this paper. Table 3 presents a comparison of values obtained in this paper for the critical load in the first mode of linear buckling with the values obtained by Sanchez et al. (2015) for laterally reinforced plates.

Type of plate	100°C	150°C	177°C
Critical load for plates with reinforcements all along the perimeter	1112 N	1430 N	1473 N
Critical load for plates with lateral reinforcements	710 N	900 N	1000 N

Table 3: Comparison between plates with different type of reinforcements.

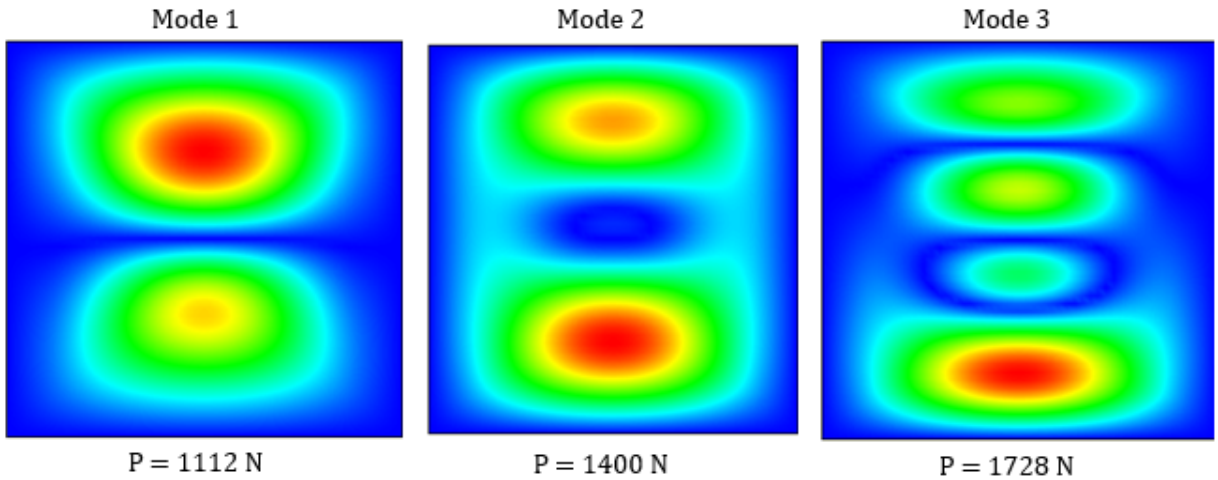

Figure 10: Modal shapes of buckling for 100°C, P is the critical load.

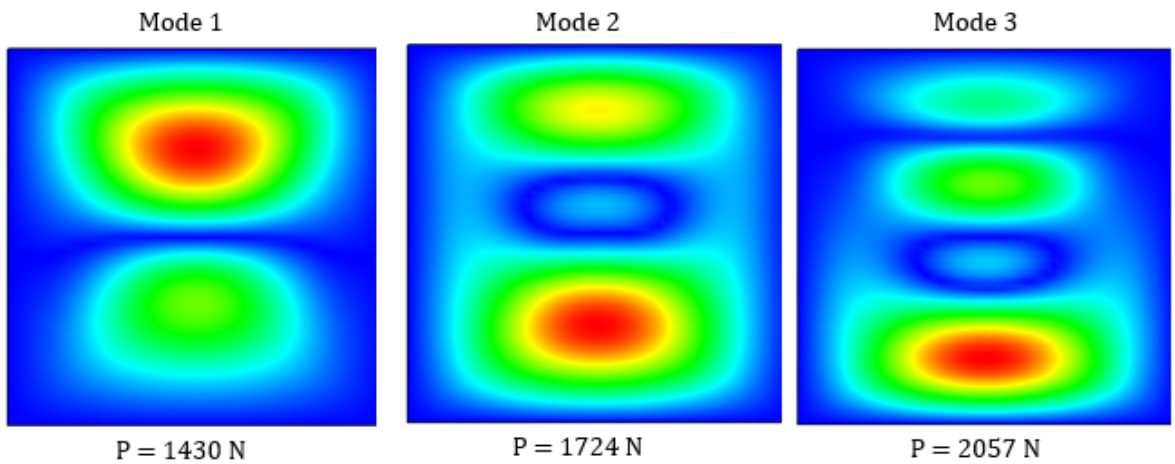

Figure 11: Modal shapes of buckling for 150°C, P is the critical load.

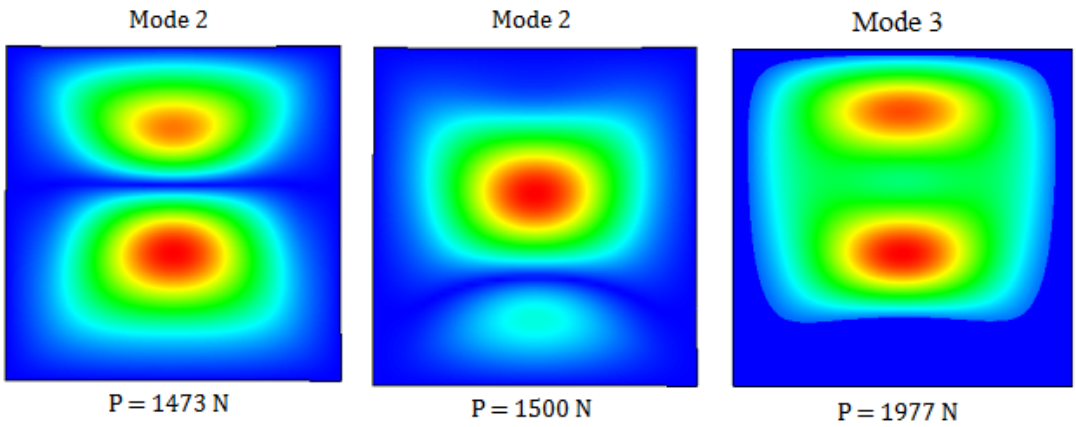

Figure 12: Modal shapes of buckling for 177°C, P is the critical load.

5.2 Post-Buckling State

For the experimental analysis of the post-buckling stage, the plates were subjected to compressive loading. This test consisted of applying uniform displacements applied in predefined time intervals. A displacement of 2 mm at 0.2 mm intervals was applied to compress the elements. The optical equipment was used for the determination of the displacements out of the plane. Successive images can be acquired at intervals of vertical displacement equal to 0.2 mm of the load cell. The subtraction of consecutive images was performed with the aid of TPLA40012® software. This subtraction yields a third image that provides the transverse displacement, w, on the whole surface of the plate. The variation of the transverse displacement with increasing load for each plate is obtained by summing up the differences of the measured results.

The numerical model was developed considering the procedure described in section 4.The comparison between the two cases neglecting and considering residual stresses are shown in Figures13 and 14, respectively. In these figures, the first case represents an ideal plate and second case represents the model with geometrical imperfections.

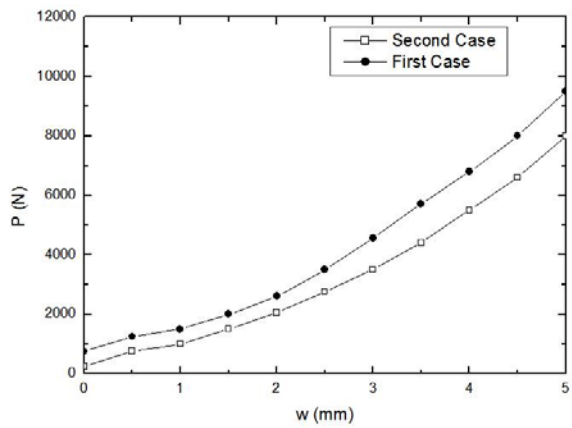

Figure 13: Comparison of numerical results for the two types of plates cured at 22°C.
P is the compression load, and w is the transverse displacement.

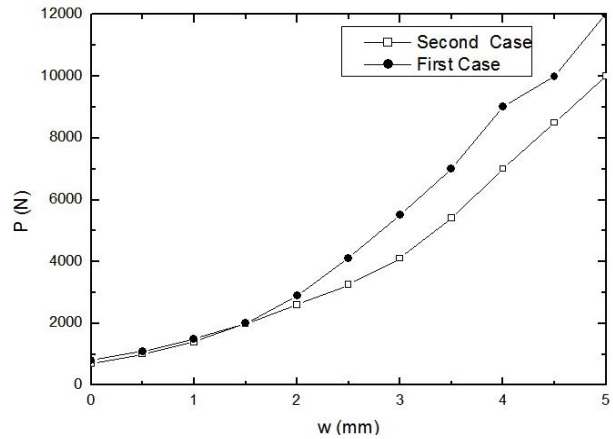

Figure 14: Comparison of numerical results for the two types of plates cured at 177°C.

P is the compression load, and w is the transverse displacement.

Figures13 and 14 provide results suitable for comparing the variation of the out-of-plane displacements with increased buckling load. This model, having asymmetric geometry, developed using CATIA® (second case), is more representative of the real conditions of the experimental study because it simulates the test conditions. For this reason, results of this study are related to the design of the plates, based on the second type of analysis. After choosing the numerical model, results can be compared with those derived from buckling tests. Figure 15 compares experimental and numerical results of the plates neglecting and considering residual stresses, respectively.

It can be stated from graphs of Figures15 and 16that the numerical results reasonably fit the experimental values. The graphs obtained from the values provided by optical equipment adequately characterize the behavior of the plates. The numerical results show that the presence of residual thermal stress causes an increase in the stiffness of the plates. Figure 17 shows results of numerical models for plates with and without residual stress. It can be observed in the figure that it can be proved that the laminate stiffness increases as the load applied.

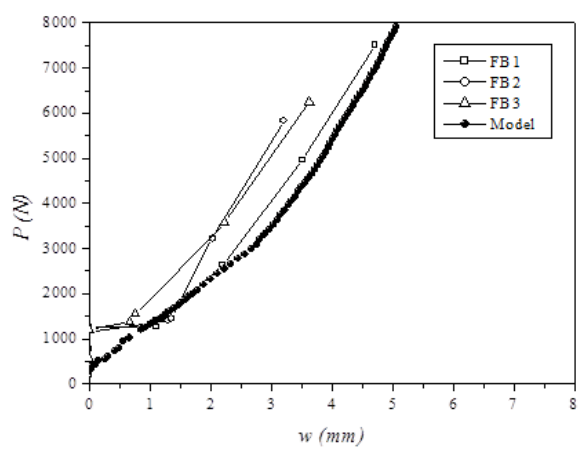

Figure 15: Post-buckling of plates cured to 22°C, P is the compression load, and w is the transversal displacement.

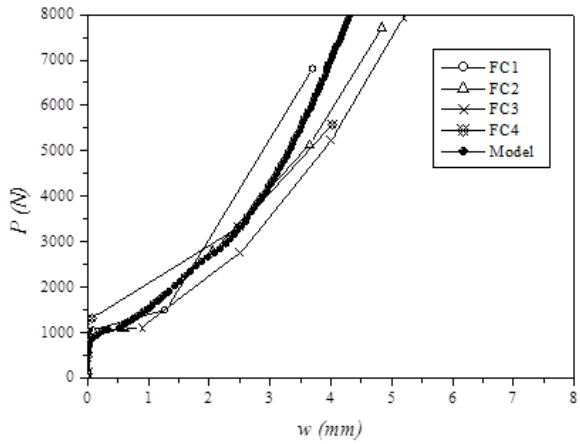

Figure 16: Post-buckling of plates cured to 177°C. P is the compression load, and w is the transversal displacement.

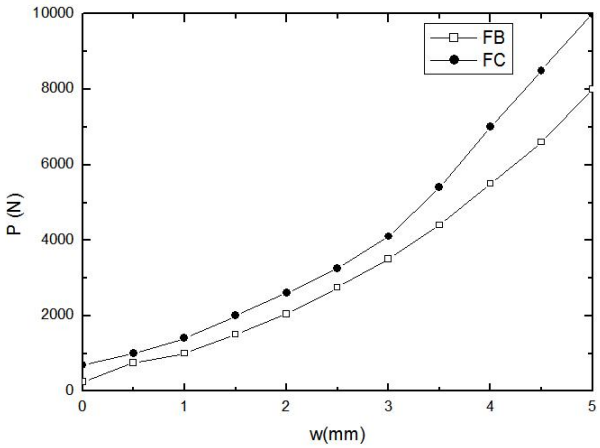

Figure 17: Results of numerical models for plates with and without residual stresses. P is the compression load, and w is the transversal displacement.

The variation of transverse displacements(w) along the horizontal axis (x) as a function of compressive loading from the numerical simulation for plates with and without thermal residual stress are shown in Figures18 and 19. When comparing the results from numerical models with experimental results, it can be observed that the displacements obtained experimentally for plates without residual stresses are greater than the displacement predicted by the model. The difference found between the experimental and numerical results could be associated with the fact that the initial conditions of each plate are different and with the possible inaccuracies in generating the conditions for support within the framework created for this purpose. The difference between numerical and experimental results varies between 12% and 18% for the loads analyzed. In the case of plates having residual thermal stress, the experimental results adequately fit the numerical model, showing a maximum error of 5%.

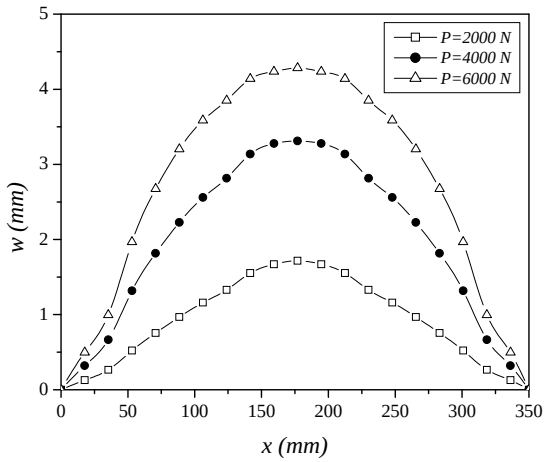

Figure 18: Variation of transverse displacement along the x axis as a function of compressive load applied to plates without thermal residual stresses.

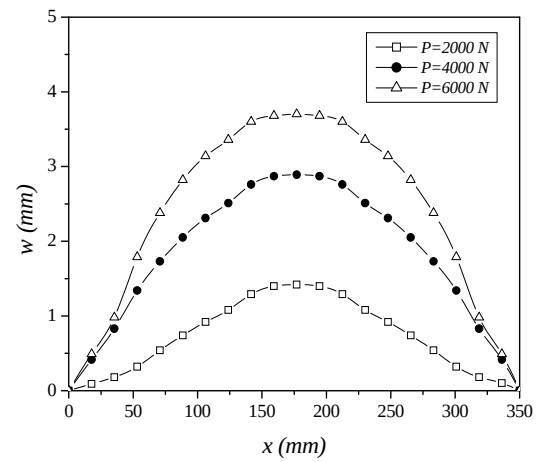

Figure 19: Variation of transverse displacement along the x axis as a function of compressive load applied to plates with thermal residual stresses.

Upon analyzing Figures 18 and 19, we can see that with increasing temperature there is an increased stiffness of the material, which can be significant when the material is in a linear regime but is clearly not exposed when the material is in a post-buckling regime. An important factor to consider is the value of the applied temperature, since it has been found that when that it increases, there comes a time when its influence on the mechanical performance of the material becomes smaller.

In the literature, reports show that there is a temperature range at which the residual thermal stresses do not play a significant role in the performance of the composite material. This information is useful for the development of new methods of optimization of the process of manufacturing of this type of material.

Aimed at assessing the effects of post buckling behavior, the variation of transverse displacement as a function of compression stresses is shown in Figure 20. For this case, the area of critical cross section was computed considering the region where the greatest distortions occur, that is, the center of the plate. The area of the critical cross section was computed as the laminate thickness (0.68 mm) times its length (354 mm).

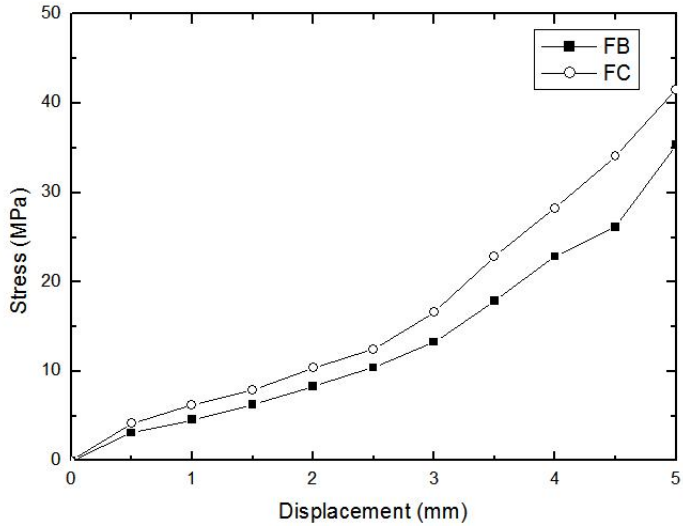

Figure 20: Variation of transverse displacement is function of stresses in post-buckling region

6 CONCLUSIONS

Many studies that can be consulted in the technical literature suggest that the effect of thermal stresses that occur during the manufacturing process of composite laminates may generate negative effects in the material, and many times cause delamination in the composite. The results submitted in this paper experimentally prove that it is possible to induce the presence of these stresses in order to improve the mechanical performance of the laminate under certain conditions of temperature. The results show that by inducing a uniform temperature field during the manufacturing process of composite laminates, not only is the value of the critical load buckling affected, but also the maximum displacements occurring in the transverse direction there of; also, mode shapes are modified. In the specific case of the load values obtained when the material is in the linear regime, these values are consistent with the results obtained by the authors of previous research, showing that it is possible to take advantage of the presence of these stresses in order to improve the performance of the composite, which could be interesting from a structural point of view.

The results obtained in the phase of post-buckling show that increasing the cure temperature increased the stiffness of the plate, proving that the temperature rise generates a non-linear increase in the stiffness of the material. Similar results are found in the consulted technical literature and can confirm what was already shown by previous studies, the possibility of using this information in the search for a suitable processing temperature of the material in order to reduce failure by buckling that often occurs in this type of material.

The software used is a powerful tool for numerical simulation. The use of "Explicit Dynamic Analysis" of ABAQUS® allows efficiently analyzing the behavior of laminates subjected to buckling , providing easy data entry and reduced processing times and reporting reliable results consistent with the values obtained experimentally.

An important contribution of this paper is the experimental methodology. The use of the optical procedure was an efficient tool in the study of the behavior of the plates analyzed. The total absence of contact between the measuring system and the measurement surface prevents undesirable alterations in reading the displacements. The simultaneous capture of many images and their processing reduces possible sources of error generated by the initial imperfections of the plate.

Acknowledgments

The authors acknowledge the financial support received for this paper from FAPESP, CNPq, and Nueva Granada Military University, UMNG.

References

Abaqus 6.5-1, (2005). Theoretical Manual, 991 p.

Aktas, M., Karakuzu, R., Arman, Y.,(2009). Compression-after impact behavior of laminated composite plates subjected to low velocity impact in high temperatures. Composite Structures. V: 89, n: 1:77–82.

Andrade, L. H., (2002) Otimização de placas laminadas com tensões residuais térmicas em problemas de estabilidade elástica e de freqüências naturais.Instituto Tecnológico de Aeronáutica, (in Portuguese), 213 p.

Andrade, L. H., Almeida, S. F. M., Hernandes, J. A., (2001) Buckling optimization of a thin composite reinforced plate with a central circular hole in the presence of thermal residual stresses. Proceeding of International Conference on Science and Technology of Composite Materials: 207-209.

Almeida, S.F.M., Hansen, J.S., (1999). Natural frequencies of composites plates with tailored thermal residual-stresses. International Journal of Solids and Structures. V: 36, n:23: 3517-3539.

Almeida, S.F.M., Hansen, J.S., (2002). Buckling of composite of plates with damage and thermal residual stresses. IAAA Journal. V: 40, n: 2: 340-345.

Almeida, S.F.M., Hansen, J.S., (1997). Enhanced buckling loads of composite plates with tailored thermal residual stresses. Journal of Applied Mechanics. V: 64, n: 4: 772-780.

Besednjak, A., (2005) Materiales Compuestos. Procesos de Fabricación de Embarcaciones. Universidad Politécnica de Cataluña, 193 p.

Donadon, M.V., Rizzi, P., Almeida, A. E., (2010). A numerical study on the post-buckling behavior of shallow singly-curved panels. Proceeding of VI National Congress Of Mechanical Engineering, 8p.

Ersoy, N., Vardar, O., (2000).Measurement of residual stresses in layered composites by compliance method. J Compos Mater. V:34: 575–598.

Fantin, A. V., (1999). Medição de formas livres tridimensionais por topogrametria Dissertação, . Dissertação de Mestrado em Engenharia Mecânica. Universidade Federal de Santa Catarina, Florianópolis (in Portuguese).

Feng, Y., He, Y., An, T., Cui, R., Shao, Q., Fan, C., (2015). Effect of hygrothermal condition on buckling and post-buckling performance of CCF300/5228A aero composite stiffened panel under axial compression. Journal of Reinforced Plastics and Composites. V: 34, n: 13:989:999.

Gascoigne, H.E., (1994) Residual surface stresses in laminated cross-ply fiber-epoxy composite materials. Exp Mech. V: 34:27–36.

Hosseini-Toudeshky, H., Mohammadi, B., (2009). Thermal residual stresses effects on fatigue crack growth of repaired panels bounded with various composite materials Compos Struct. V: 89: 216–223.

Ibekwe, P.F., Mensah, P.F. Pang, G. L.S., Stubblefield, M.A., (2007). Impact and post impact response of laminated beams at low temperatures. Composite Structures: 12-17.

Kim, J.W., Lee, J.H., Kim, H.G., Kim, H.S., Lee, D.G., (2006). Reduction of residual stresses in thick-walled composite cylinders by smart cure cycle with cooling and reheating. Compos Struct. V: 75:261–266.

Kim, H.S., Yoo, S.H., Chang, S.H., (2013). In situ monitoring of the strain evolution and curing reaction of composite laminates to reduce the thermal residual stress using FBG sensor and dielectrometry. Compos Part B: Eng. V: 44, n1:446-452.

Nabaei, S.S., Baverel, O., Weinand, Y., (2013).Mechanical form-Finding of the Timber Fabric Structures with Dynamic Relaxation Method. International Journal of Space Structures. V: 28, n3:1:19.

Nunes, F.M., (2005).Análise da pós-flambagem de placas de material compósito na presença de tensões residuais térmicas. Tese de Mestrado em Engenharia Mecânica e Aeronáutica. Instituto Tecnológico de Aeronáutica, São José dos Campos (in Portuguese).104 p.

Nunes, F.M., Almeida, S.F.M., (2005). Post-buckling analysis of composites material plates in presence of thermal residual stresses. Proceeding of 18th International Congress of Mechanical Engineering, 8p.

Palerosi, A.C., (2006). Avaliação do comportamento termomecânico de laminados em material compósito por processmento digital de imagens. Tese de Doutorado em Engenharia Mecânica e Aeronáutica. Instituto Tecnológico de Aeronáutica, São José dos Campos (in Portuguese). 247 p.

Parlevliet, P.P., Bersee, H.E.N., Beukers, A., (2006). Residual stresses in thermoplastic composites—A study of the literature. Part I: Formation of residual stresses. Composites. Part A: Applied Science and Manufacturing. V: 37:1847-1857.

Pradhan, B., Panda, S. K., (2006). Characterization of Curing Stress Effects on Fracture Behavior of FRP Laminated Compo-sites with Embedded Delaminations. Journal of Reinforced Plastics and Composites. V: 25, n: 17:1847-1864.

Sánchez, M.L., Almeida, S.F., (2007). Experimental characterization of thermal residual stresses on the stiffness of composites plates. Proceedings of 19th International Congress of Mechanical Engineering, Brazil. 9p.

Sánchez, M.L., Carrillo, J., Almeida, S.F.M., (2015). Evaluación de las tensiones térmicas residuales en el pandeo y post-pandeo de placas con refuerzos laterales. Preprint submitted to Revista Latinoamericana de Metalurgia y Materiales, 24p.

Shokrieh, M.M., Daneshvar, A., Akbari. S., (2014). Reduction of thermal residual stresses of laminated polymer composites by addition of carbon nanotubes. Materials and Design. V: 53:209-216.

Tay, T.E., Shen, F., (2002). Analysis of delamination growth in laminated composites with consideration for residual thermal stress effects. J Compos Mater. V: 36 , n:11:1299–1320.

Taylor, M., Davidovitch, B., Qiu, Z. , Bertoldia, K., (2014). A comparative analysis of numerical approaches to the mechanics of elastic sheets, Preprint submitted to Journal of the Mechanics and Physics of Solids, 23p.